RSC Advances

PAPER

View Article Online
View Journal | View Issue

Cite this: *RSC Adv.*, 2019, **9**, 435

Dimethylacrylamide, a novel electrolyte additive, can improve the electrochemical performances of silicon anodes in lithium-ion batteries

Guobin Zhu, Siming Yang, Yan Wang, Qunting Qu* and Honghe Zheng*

Received 26th September 2018
Accepted 29th November 2018

DOI: 10.1039/c8ra07988a

rsc.li/rsc-advances

To enhance the electrochemical properties of silicon anodes in lithium-ion batteries, dimethylacrylamide (DMAA) was selected as a novel electrolyte additive. The addition of 2.5 wt% DMAA to 1.0 M $LiPF_6$/EC : DMC : DEC : FEC (3 : 3 : 3 : 1 weight ratio) electrolyte significantly enhanced the electrochemical properties of the silicon anode including the first coulombic efficiency, rate performance and cycle performance. The solid electrolyte interphase (SEI) layers developed on the silicon anode in different electrolytes were investigated by a combination of electrochemical and spectroscopic studies. The improved electrochemical performances of the Si anode were ascribed to the effective passivation of DMAA on the silicon anode. The addition of DMAA helped develop a uniform SEI layer, which prevented side reactions at the interface of silicon and electrolyte.

1. Introduction

High-performance lithium-ion batteries (LIBs) are very important to support the rapid growth of power and battery technologies. Graphitic carbon cannot meet the requirements of high energy density due to its relatively low capacity (372 mA h g^{-1}).[1,2] Many promising anode materials such as Si-based, tin-based or other metal-based materials with improved volume and weight energy density have been extensively studied in recent years.[3–6] Among them, silicon has attracted attention because of its high specific capacity of 4200 mA h g^{-1}, comparably low delithiation potential of 0.4 V, rich reserves, acceptable cost and environmental friendliness.[7,8] However, silicon undergoes a dramatic volume change (around 300% for $Li_{4.4}Si$) during Li^+ insertion and extraction, which makes the solid electrolyte interphase (SEI) highly unstable. At a low electrode potential, the electrolyte components reductively decompose and build up a passivating SEI layer on the silicon surface.[9] In contrast with that on graphite, the SEI development on the Si surface is always incomplete and fragile. As the Si particle expands and contracts, it easily cracks, breaks off and forms fluffy debris. Regrowth and rearrangement of SEI on an Si anode are accompanied by continuous consumption of active lithium and electrolyte. Therefore, SEI optimization is very critical for developing high-performance LIBs with Si anodes.

To date, many attempts have been reported including reducing the particle size of silicon and developing many new binders for improving the mechanical properties as well as maintaining conductive passages of silicon electrodes.[10–16] Although these solutions are quite effective, there are still some major problems for Si anode: large irreversible capacity loss, poor rate capability and cyclability. One of the main obstacles is the instability of the SEI layer. On the one hand, the continuous rupture and regrowth of SEI resulting from large volume changes block Li-ion diffusion and increase the electronic resistance of the electrode. On the other hand, the growth of the SEI layer traps increasing amounts of active lithium, which causes serious irreversible capacity deterioration.[17,18] To improve the SEI quality on Si anodes, addition of film-forming additives in the electrolyte is a prevalent strategy because they can advance the formation of uniform SEI layers on the silicon particle surface. This effect occurs at higher potentials than that with ordinary carbonate electrolytes. Some of the film-forming additives for graphite anodes are also effective for Si anodes. Vinyl carbonate (VC),[19] fluoroethylene carbonate (FEC),[20–22] succinic anhydride (SA)[23,24] and lithium bis(oxalato)borate (LiBOB)[25] have been proven to be effective for silicon anodes. Nowadays, FEC is widely adopted in electrolyte solutions with Si anodes.[15,20–22,26–35] The main products of FEC decomposition on the electrode are known to be $ROCO_2Li$, LiF and polymerized FEC. These products contribute to a uniform and stable SEI layer on the silicon particle surface, thereby preventing further decomposition of EC and $LiPF_6$ salts at lower potential conditions. Nevertheless, the effect of FEC additive in electrolyte is still far from satisfactory in stabilizing the electrode surface and reducing the rupture of SEI. LiBOB additive generates a higher content of oxalates and $Li_xPF_yO_z$. However, the lower LiF content in the SEI film results in modest improvement of the cycling stability for Si anodes.[25] Han *et al.*[23] confirmed that there is high content of hydrocarbon and Li_2CO_3 on the silicon

College of Energy & Collaborative Innovation Center of Suzhou Nano Science and Technology, Soochow University, Suzhou, Jiangsu, 215006, P. R. China. E-mail: qtqu@suda.edu.cn; hhzheng@suda.edu.cn

surface with the additive of SA. Li *et al.*[24] confirmed that SA can prevent further dissociation of $LiPF_6$ in the electrolyte, which improves the electrochemical performance of Si/C nanofibers. Aurbach *et al.*[36] proved that amorphous Si anodes are compatible with ionic liquid electrolytes based on derivatives of piperidinium-TFSI molten salts. Chen *et al.*[19] found that VC additives contribute to the growth of a polyvinylene carbonate-based uniform SEI layer on silicon anodes and thus improve the heat stability of 1.1 M $LiPF_6$ EC/EMC electrolyte. In spite of this, film-forming additives for Si anode are still very rare. The development of novel and effective film-forming additives for Si is very important for the application of Si anodes in high-performance LIBs.

N,*N*-Dimethylacrylamide (DMAA) is a type of acrylamide monomer, which dissolves well in many organic and aqueous solvents due to its typical hydrophilic and hydrophobic groups. DMAA has unsaturated functional groups and an amide group with a super conjugation system between the nitrogen, carbonyl and double bonds. DMAA can be reduced and forms effective SEI films on Si surfaces prior to lithiation of Si anodes, thus inhibiting further decomposition reactions of the electrolyte. Moreover, DMAA forms a complex with the Lewis acid PF_5 produced by the thermal dissociation of $LiPF_6$ and can prevent the decomposition of $LiPF_6$ electrolytes, which prevents the growth of reactive surface species that weaken the SEI layer.[37–41] Wieczorek *et al.* studied the morphology, submicrostructures and conductivity of polyether–poly(DMAA)–$LiClO_4$ electrolytes. They found that the ambient and subambient temperature conductivities can be increased by about 1 order of magnitude with fortified poly(DMAA) compared to polyether-based electrolytes.[42,43] To the best of our knowledge, the film-forming behavior of DMAA as an electrolyte additive with an Si anode has never been reported.

In this study, we report the use of a novel electrolyte additive, DMAA, with an Si anode in a commercial 1 M $LiPF_6$/EC : DMC : DEC : FEC (3 : 3 : 3 : 1) electrolyte, which is referred to as the original electrolyte in this manuscript. The most important electrochemical properties of the silicon anode including the first coulombic efficiency, rate performance and cycle performance are simultaneously enhanced. Further improvement of the electrochemical properties of silicon anodes in the electrolyte containing FEC is critical for electrolyte optimization. The SEI mechanisms of the Si anode in the electrolyte without and with different amounts of DMAA additive are discussed.

2. Experimental

2.1 Electrolyte preparations

Different solvents of ethylene carbonate (EC), fluoroethylene carbonate (FEC), dimethyl carbonate (DMC), diethyl carbonate (DEC) and lithium salt $LiFP_6$ were purchased from Capchem Technology Co. Ltd., China. Dimethylacrylamide (DMAA 99.5%) was purchased from Alfa Aesar China Co. Ltd. Before use, the DMAA solvent was pretreated by adding several clean lithium sheets under 40 °C for 24 h to remove possible reactive impurities. To prepare the electrolyte solutions, the basic solvent consisting of EC : DMC : DEC : FEC (3 : 3 : 3 : 1) was mixed in an argon-filled glove box. Thereafter, different weight ratios of DMAA were introduced into the mixing solvent. Finally, 1 M $LiFP_6$ salt was added into the above solvent. The electrolytes with DMAA additives of 1 wt%, 2.5 wt%, 5 wt% and 10 wt% are named D1, D2, D3 and D4, respectively. The conductivity of the prepared electrolytes was measured at 25 °C using a DDS-307A conductivity meter.

2.2 Electrode preparations and electrochemical testing

Silicon nano-particles (100 nm, 99.99%) were obtained from the Kejing Star Technology Co. Ltd., China. Sodium alginate with medium viscosity was purchased from Sigma-Aldrich Co. Ltd. and was used as the electrode binder in this work. Carbon conductive additive (40 nm) was acquired from TIMCAL (Switzerland). The silicon nanoparticles, carbon black, and sodium alginate binder were mixed with deionized water at a weight ratio of 70 : 15 : 15. The slurry was mixed well with a high speed shearing machine (Fluko, FA-25) at 10 000 rpm for 30 min. Afterwards, the slurry was coated onto a 15 μm-thick copper foil (99.99% purity) and dried at 70 °C for 4 h. The silicon anode was cut into small circles with a slicer and was fully dried at a temperature of 120 °C and a heating time of 12 hours with vacuum treatment. We carefully controlled the loading of the silicon active material to be 0.5 mg cm^{-2}.

Silicon electrodes were transferred into an argon-filled glove box and assembled in CR2032 coin-type half cells with a counter electrode (lithium foil), separator (Celgard 2500) and prepared electrolyte. The charge–discharge characteristics of the silicon electrodes were studied using battery test equipment (CT2001A, LAND). The formation and testing of half cells involved cycling between 0.01 and 1 V under different cycle rates of 0.05C and 0.2C, respectively. The silicon electrodes in different electrolytes were investigated by a cyclic voltammetry test and electrochemical impedance spectra obtained by an electrochemical workstation (VSP, Biologic).

2.3 Material characterization

Morphologies of the silicon electrodes cycled in the electrolytes with different amounts of DMAA additive were observed by using SEM (SU8010, Hitachi). The cycled electrodes were adequately cleaned with the organic solvent DMC and fully dried at a temperature of 40 °C and heating time of 2 hours along with vacuum treatment before the morphology test. The organic group of cycled silicon electrodes was evaluated using attenuated total reflectance mode of Fourier-transform IR spectroscopy (Tensor 27, Bruker). The elementary information on the surface of cycled electrodes was obtained by X-ray photoelectron spectroscopy (ESCALAB 250Xi, Thermo Fisher).

3. Results and discussion

DMAA additive is well soluble in the original electrolyte and mixed into clear solutions. The ionic conductivities of the prepared electrolyte and 1 M $LiPF_6$/DMAA solution are compared in Fig. 1. A slight increase in the ionic conductivity is

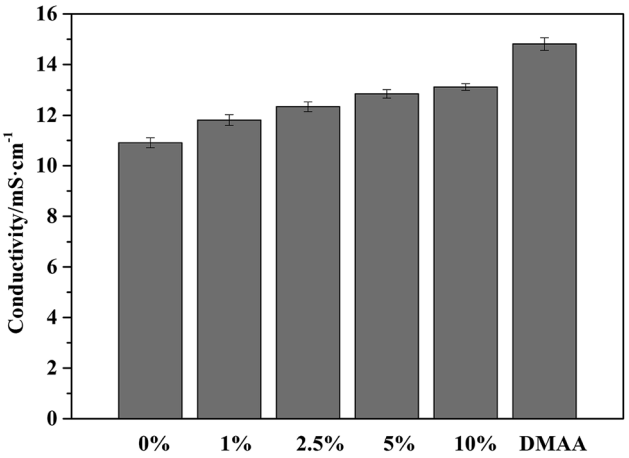

Fig. 1 Conductivity of 1 M $LiPF_6$/EC : DMC : DEC : FEC (3 : 3 : 3 : 1) electrolytes with different contents of DMAA additive and 1 M $LiPF_6$/DMAA.

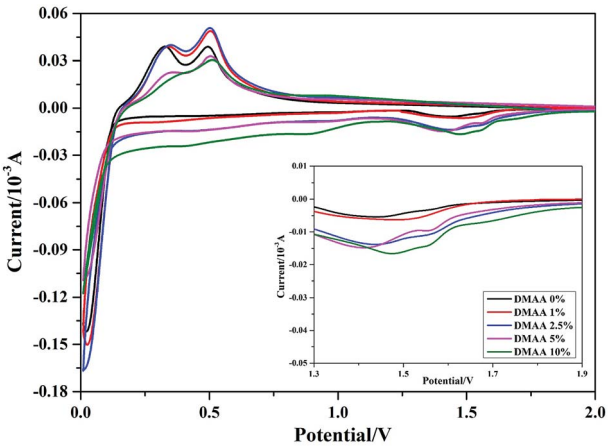

Fig. 3 Cyclic voltammetry profiles of the silicon anode in 1 M $LiPF_6$/EC : DMC : DEC : FEC (3 : 3 : 3 : 1) electrolytes with different contents of DMAA additive (scan rate: 0.05 mV s^{-1}).

obtained with increasing DMAA concentration in the electrolyte. This result is explained by the higher DN value (DN = 26.6) of DMAA compared to that of DMC and DEC solvents.[44,45] Therefore, the preferential solvation of Li^+ to DMAA molecules and the reduced Stokes radius of Li^+ in the solution contribute to enhancement of the ionic conductivity.[46]

The cyclic voltammetry of the Si anode in 1 M $LiPF_6$/DMAA solution is shown in Fig. 2. DMAA is reduced at around 1.5 V *vs.* Li/Li^+ during the first negative scanning process. The 1.5 V potential is notably higher than the reduction potential of the main solvents EC, DMC, DEC and FEC.[47] At this potential, DMAA is decomposed on the Si surface and thereby builds up a passivation film prior to the decomposition of the main solvents. The strong reduction peak at 1.5 V vanishes in the second cycle, implying that the Si anode is effectively passivated by the reduction reactions of DMAA at the interface of silicon and electrolyte. Therefore, DMAA can function as a valid film-forming additive with the Si anode.

Fig. 3 displays the cyclic voltammetry of the silicon anode in different electrolytes in the first cycle. The reduction peak in the first negative scanning process appears at around 1.6 V *vs.* Li/Li^+, corresponding to SEI development on the Si surface. The onset potential associated with the irreversible reduction is shifted to a higher potential after adding more DMAA additive. Meanwhile, an increase in the peak intensity with increasing DMAA content is observed, implying that DMMA is reduced before the decomposition of carbonate solvents. The cathodic peak is near 0 V and is ascribed to lithiation of the Si anode.[29,32] In the following anodic process, the value of anodic peak of the Si anode slightly increases after addition of 1 wt% and 2.5 wt% DMAA additives in the electrolyte. However, at a high content of DMAA (5 wt% to 10 wt%), a significant reduction in the 0.3 V delithiation peak represents an increase in the electrode polarization, implying that a thick passivation film has developed.[48]

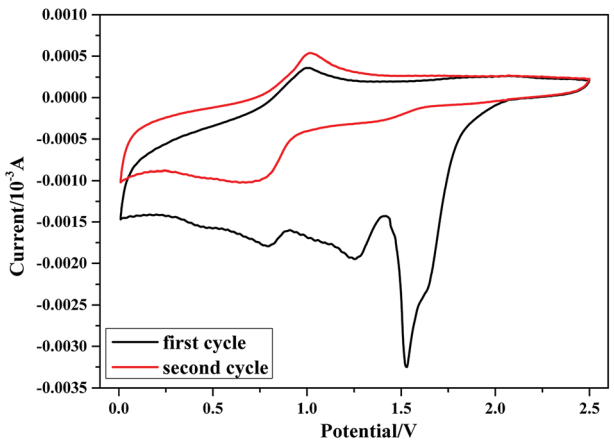

Fig. 2 Cyclic voltammetry profiles of the silicon anode in 1 M $LiPF_6$/DMAA.

Fig. 4 displays the first charge–discharge curve of the silicon anode cycle with different electrolytes. Compared to the result for the original electrolyte, a potential plateau at about 1.3 V is due to the decomposition reaction of DMAA molecules. With increasing content of DMAA in the electrolyte, the potential plateau is prolonged, and the plateau at around 0.75 V associated with the reduction reaction of Li-solvated EC molecules is reduced.[27,28] Meanwhile, the potential plateau at around 0.1 V corresponding to the lithiation of the Si anode is prolonged.[6,9] The initial charging and discharging specific capacities are 4435.1 and 3500.3 mA h g^{-1}, respectively, corresponding to the first coulombic efficiency of 78.92% in the original electrolyte; by comparison, for D2, the values are 4572.1 and 3665.0 mA h g^{-1}, corresponding to the first coulombic efficiency of 80.16%. However, the reversible capacity and coulombic efficiency decrease when the content of DMAA is further increased, which may be associated with the strong decomposition reaction of DMAA at the interface. A thick and dense passivation film developed on Si surface must affect its electrochemical properties.[49] In this study, the optimum content of DMAA in the electrolyte is determined to be 2.5 wt% for the Si anode.

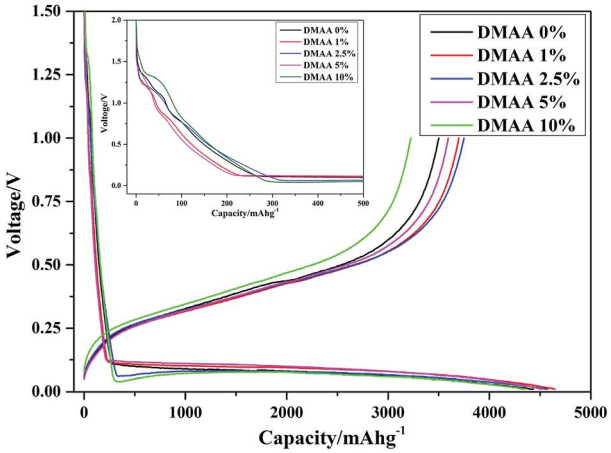

Fig. 4 Charge–discharge profiles for first cycle of the Si anode in 1 M $LiPF_6$/EC : DMC : DEC : FEC (3 : 3 : 3 : 1) electrolytes with different contents of DMAA additive.

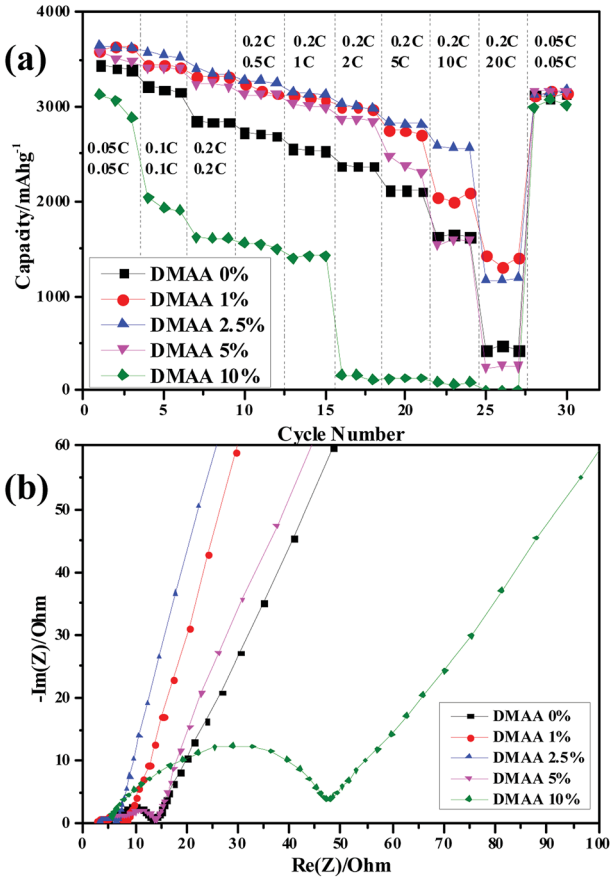

Fig. 5 (a) Rate capability and (b) Nyquist plots of the silicon electrode in 1 M $LiPF_6$/EC : DMC : DEC : FEC (3 : 3 : 3 : 1) electrolytes with different contents of DMAA additive.

The rate performance of the silicon anode cycle with different electrolytes was investigated at nine different rates ranging from 0.05 to 20C. The discharge capacity values of the silicon anode in the original electrolyte at 1C, 5C and 20C are

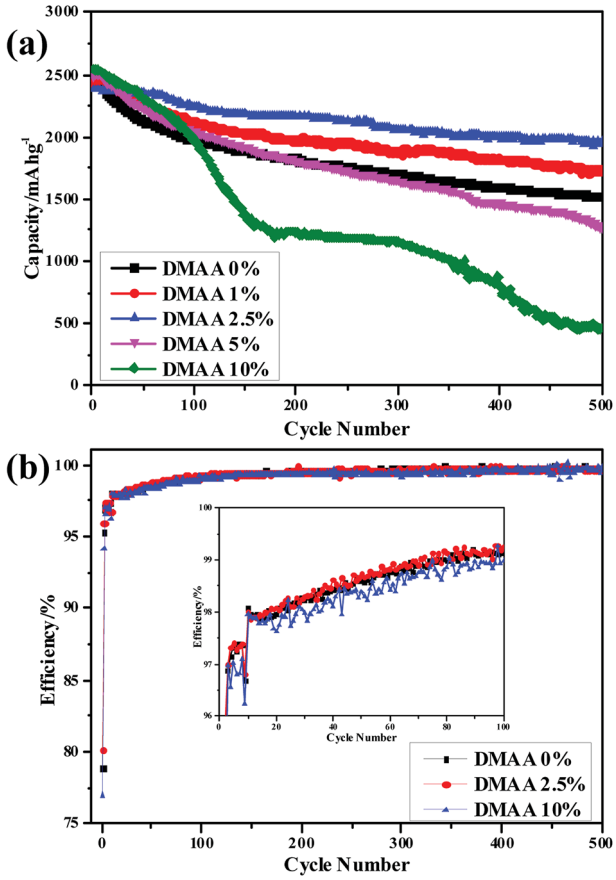

Fig. 6 (a) Cycling comparison and (b) coulombic efficiency of the silicon anode in 1 M $LiPF_6$/EC : DMC : DEC : FEC (3 : 3 : 3 : 1) electrolytes with different contents of DMAA additive.

2554.9, 2115.2 and 420.1 mA h g^{-1}, corresponding to the capacity retentions of 74.3%, 61.5% and 12.2% (Fig. 5a). In contrast, the addition of 1 wt% and 2.5 wt% DMAA results in significant enhancement in the rate capability of the silicon anode. Particularly for D2, the Si anode achieves discharge capacity of 1162.4 mA h g^{-1} at the rate of 20C, corresponding to capacity retention of 31.8%. The significantly enhanced rate capability of the Si anode is due to the optimization and modification of the SEI layer by addition of a proper amount of DMAA in the electrolyte.[19] This can be confirmed by the electrochemical impedance spectroscopy (EIS) results, which were measured after the rate performance test. The EIS values of the silicon electrodes at a depth of charge of 65% after rate test in the mixed electrolytes are compared (Fig. 5b). The first small semicircle in the high-frequency region represents low resistance of the silicon particles (R_{SEI}).[18,32] The second semicircle appears in the medium-frequency region, which can be correlated to the charge transfer resistance of the silicon electrode surface (R_{ct}). By comparison, the electrode impedance decreases in the presence of a small amount of the DMAA additive. With the addition of 2.5 wt% DMAA, the lowest R_{SEI} and R_{ct} values are obtained, which explains the improved rate performance of the silicon electrode. Further increasing the DMAA content causes significant increase in electron transfer impedance related to

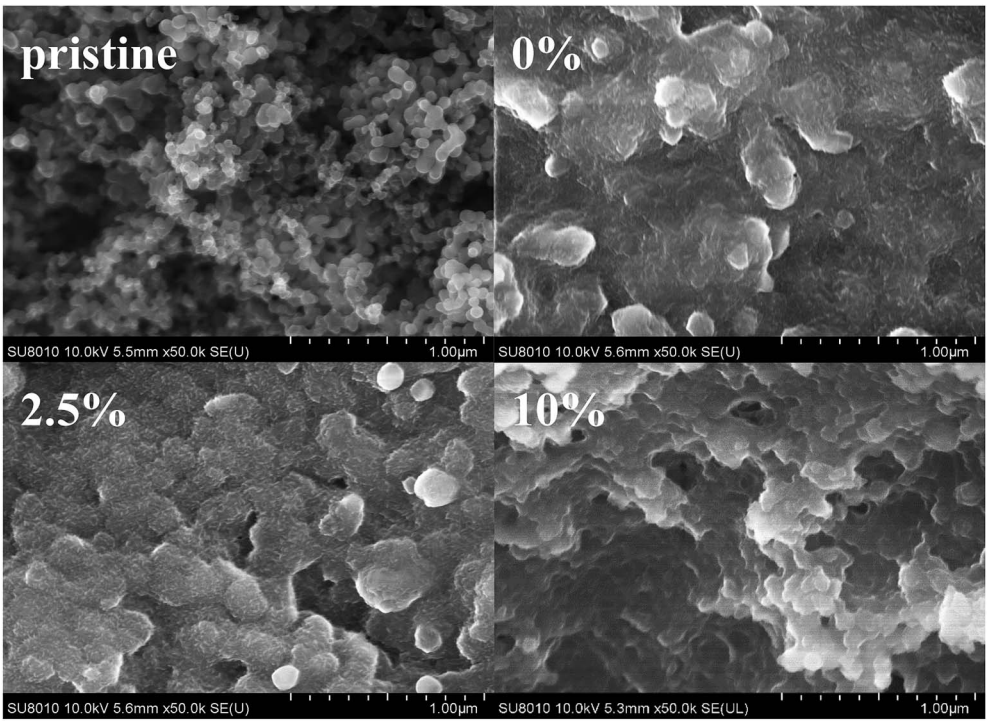

Fig. 7 SEM images of the silicon anode after 500 cycles in the electrolytes with different contents of DMAA additive at current of 0.84 A g^{-1}.

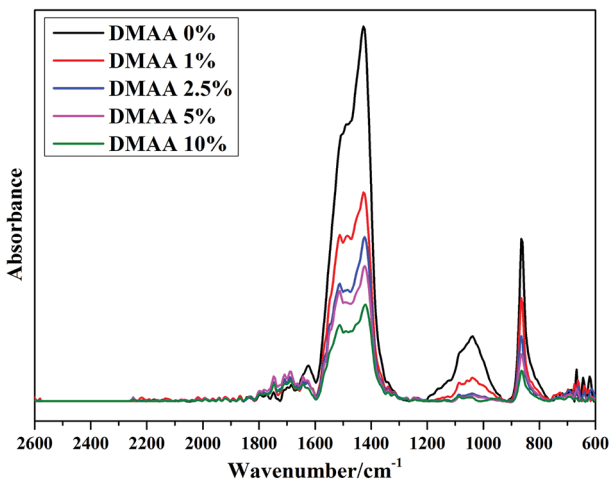

Fig. 8 FTIR spectra of the silicon electrode after 500 cycles with 1 M $LiPF_6$/EC : DMC : DEC : FEC (3 : 3 : 3 : 1) electrolytes with different contents of DMAA additive.

the strong reduction of DMAA molecules at the interface of silicon and electrolyte, which affects the diffusion of Li ions.

The cycle performance of the silicon anode cycled with different electrolytes was evaluated at a current density of 0.84 A g^{-1} (0.2C). As shown in Fig. 6a, upon galvanostatic charge–discharge cycling, the reversible capacity of the Si anode without DMAA exhibits rapid capacity fading from 2467.6 to 1522 mA h g^{-1} in 500 cycles, corresponding to ~40% capacity loss. By comparison, the Si anode showed higher capacity retention in the electrolyte in the presence of a proper amount of DMAA additive over prolonged cycling process. After 500 cycles, the Si anode delivered reversible capacities of 1734.1, 1950.7, 1274 and 466.3 mA h g^{-1} in D1, D2, D3 and D4, respectively. The capacity loss of the Si anode in D2 is less than 20%. More importantly, the Si anode in D2 displayed high coulombic efficiency over the whole cycling process. In Fig. 6b, we have compared the coulombic efficiencies of the Si anode cycled with the original electrolyte, D2 and D4 in the initial 100 cycles. Enhancement in the coulombic efficiency is obtained by the addition of 2.5 wt% DMAA additive, but clear deterioration is seen with the addition of 10 wt% DMAA additive.

We observed the morphologies of the silicon anode before and after 500 cycles in different electrolytes (Fig. 7). The surface of pristine silicon nanoparticles is clean and smooth. The solid electrolyte interface formed in the original electrolyte has non-homogeneous, rougher and more porous morphology. By comparison, the silicon electrode cycled with D2 shows smooth and uniform morphology. Many silicon particles disintegrate when cycled in D4. These morphology images clearly indicate that a proper amount of DMAA can effectively protect the silicon anode in the carbonate original electrolyte. SEI produced with the proper amount of DMAA is uniform, compact and resistant to the decomposition of the electrolyte and fracture of silicon particles.[50]

FTIR spectra (Fig. 8) recorded from silicon electrodes after the cycling test provide information about the surface chemistry. The broad peaks in the 1200–900 cm^{-1} range in the original electrolyte are associated with asymmetric –COO–, symmetric –COO– and asymmetric C–O–C vibrations.[51] Suppression of the 1200–900 cm^{-1} range by addition of DMAA additive indicates the surface modification of the Si nano-

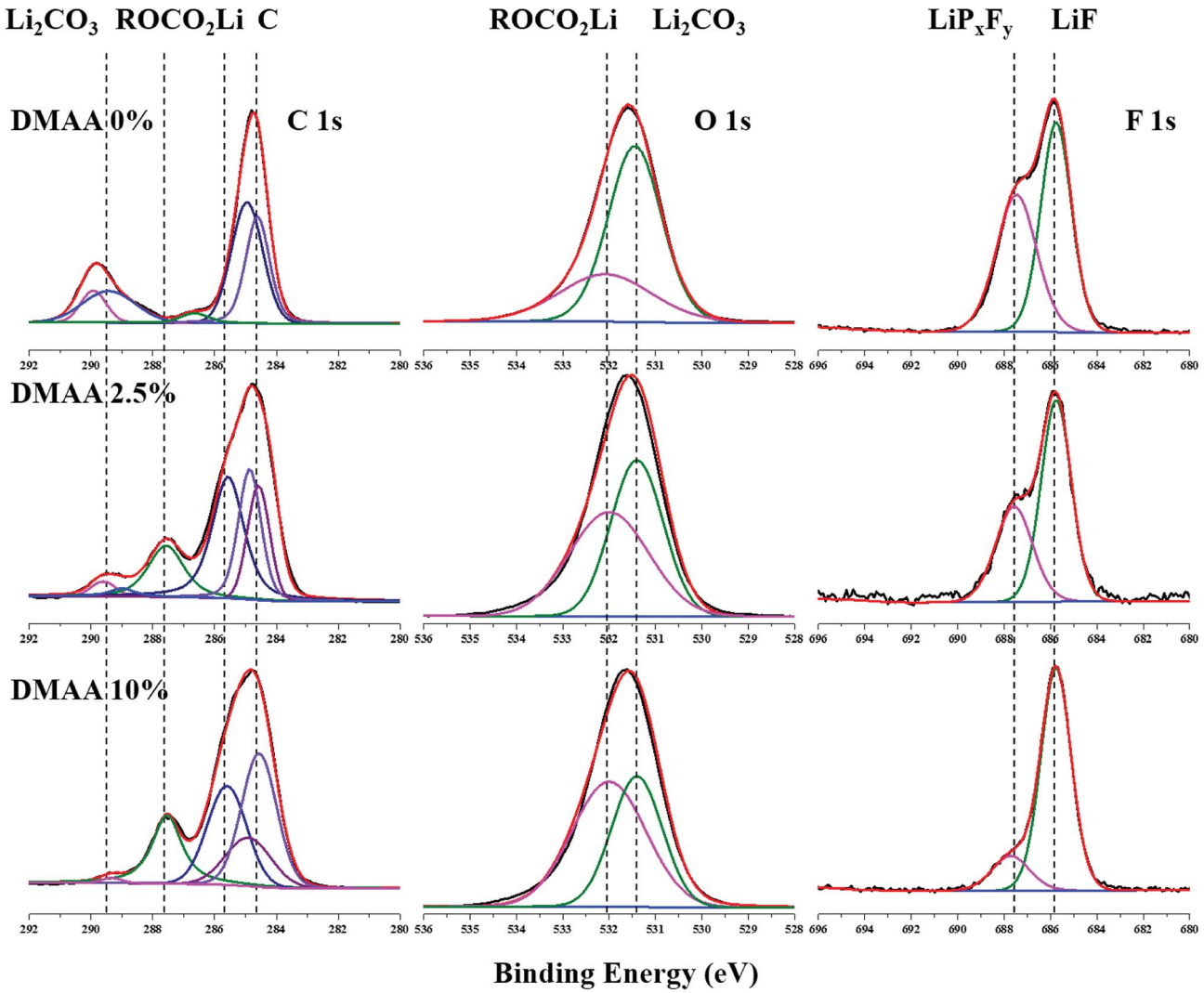

Fig. 9 XPS spectra for silicon electrode C 1s, O 1s and F 1s after 500 cycles with 1 M $LiPF_6$/EC : DMC : DEC : FEC (3 : 3 : 3 : 1) electrolytes with different contents of DMAA additive.

particles. Meanwhile, the strong vibrations of the $OCOO^-$ moiety of Li_2CO_3 at 1512, 1427 and 864 cm^{-1} can be found for all electrodes.[13] The intensity of the typical Li_2CO_3 peaks is reduced with increase in DMAA additive, indicating that the decomposition of the main solvent is suppressed. The typical peaks between 1643 and 1747 cm^{-1} are not very prominent for the original electrolyte, which should be ascribed to poly(-DMAA) species.[42] The intensity of the broad peak significantly increases after the addition of DMAA additive; this is due to the double bond in DMAA, which makes the additive more electrochemically active on the Si surface.

To gain deeper insights into the mechanisms of the DMAA additive, the harvested Si anodes after the cycling test were analyzed by XPS. Fig. 9 shows the XPS spectra of C 1s, O 1s and F 1s for the Si surfaces developed in different electrolytes. For the original electrolyte, the typical peak related to Li_2CO_3 at 289.9 eV (CO_3) in the C 1s spectrum and the C=O peak at 531.4 eV in the O 1s spectrum are observed. The intensity of the Li_2CO_3 peak is reduced by addition of DMAA additive. The typical peaks related to $ROCO_2Li$ appear at 287.7 eV (CH_2O) and 285.8 eV (CH_2CH_2O) in the C 1s spectrum and the C=O peak is observed at 532.1 eV in the O 1s spectrum. The intensity of the $ROCO_2Li$ peak increases after the addition of DMAA additive. The clear peak in the C 1s spectrum at 284.6 eV can be ascribed to the absorbed carbon from the environment. The other peak at 285.0 eV is assigned to the alginate binder. Meanwhile, the peaks at 287.5 eV (CH_2O) and 285.6 eV (CH_2CH_2O) indicate the participation of DMAA in SEI formation with higher alkyl lithium carbonate and lower Li_2CO_3 contents. DMAA has considerable effects on the reactions of the silicon anode with the electrolyte. DMAA is more reactive compared to the carbonate solvents in the electrolyte because of double bonds.

The F 1s spectra indicate a peak at 685.7 eV (LiF) for all electrolyte samples in the experiment. The peak at 687.5 eV ($LiPF_6$ and LiP_xF_y) in the F 1s spectrum gradually decreases with the increase in DMAA content, revealing that the SEI layer mainly contains less stable salts such as LiP_xF_y in the original electrolyte. In contrast, in the original electrolyte, more LiF salt

is present on the surface layer. The weaker shoulder at 687.5 eV indicates that DMAA effectively hinders the decomposition of $LiPF_6$ salt with cycles.

4. Conclusions

In summary, we report a novel electrolyte additive, DMAA, for use with Si anode in this study. The presence of DMAA helps to develop a more stable SEI layer on the Si surface at relatively high electrode potential and thereby suppresses the decomposition reactions of the main electrolyte solvents. The significance of this study is that the electrochemical properties of silicon anode in electrolyte containing FEC can be further improved by the addition of DMAA additive. With 2.5 wt% DMAA in the 1 M $LiPF_6$/EC : DMC : DEC : FEC (3 : 3 : 3 : 1) electrolyte, the electrochemical properties of the Si anode including the first coulombic efficiency, rate performance and cycle performance are significantly enhanced. The silicon anode can maintain more than 80% of its reversible capacity after 500 cycles. The electrochemical enhancement of the Si anode results from different SEI mechanisms due to the addition of DMAA additive. The presence of DMAA enables the development of the SEI film on the Si anode at a higher electrode potential and thus mitigates the decomposition of the electrolyte solvents. Relatively low electrode impedance and compact SEI layer can be achieved by adding 2.5 wt% DMAA additive, which explains the electrochemical enhancement of the Si anode.

Conflicts of interest

The authors declare there is no conflicts of interest regarding the publication of this paper.

Acknowledgements

The authors are very grateful to the funding of the National Natural Science Foundation of China (NSFC no. 21875154 and 21473120).

References

1 S. Choi, T. W. Kwon, A. Coskun and J. W. Choi, Highly elastic binders integrating polyrotaxanes for silicon microparticle anodes in lithium ion batteries, *Science*, 2017, **357**, 279–283.
2 I. Kovalenko, B. Zdyrko, A. Magasinski, B. Hertzberg, Z. Milicev, R. Burtovyy, I. Luzinov and G. Yushin, A Major Constituent of Brown Algae for Use in High-Capacity Li-Ion Batteries, *Science*, 2011, **334**, 75–79.
3 X. X. Zuo, J. Zhu, P. Muller-Buschbaum and Y. J. Cheng, Silicon based lithium-ion battery anodes: a chronicle perspective review, *Nano Energy*, 2017, **31**, 113–143.
4 K. Eom, J. T. Lee, M. Oschatz, F. X. Wu, S. Kaskel, G. Yushin and T. F. Fuller, A stable lithiated silicon-chalcogen battery *via* synergetic chemical coupling between silicon and selenium, *Nat. Commun.*, 2017, **8**, 13888.
5 N. Kim, S. Chae, J. Ma, M. Ko and J. Cho, Fast-charging high-energy lithium-ion batteries *via* implantation of amorphous silicon nanolayer in edge-plane activated graphite anodes, *Nat. Commun.*, 2017, **8**, 812.
6 W.-J. Zhang, A review of the electrochemical performance of alloy anodes for lithium-ion batteries, *J. Power Sources*, 2011, **196**, 13–24.
7 Y. Jin, S. Li, A. Kushima, X. Zheng, Y. Sun, J. Xie, J. Sun, W. Xue, G. Zhou, J. Wu, F. Shi, R. Zhang, Z. Zhu, K. So, Y. Cui and J. Li, Self-healing SEI enables full-cell cycling of a silicon-majority anode with a coulombic efficiency exceeding 99.9%, *Energy Environ. Sci.*, 2017, **10**, 580–592.
8 R. S. Fu, K. L. Zhang, R. P. Zaccaria, H. R. Huang, Y. G. Xia and Z. P. Liu, Two-dimensional silicon suboxides nanostructures with Si nanodomains confined in amorphous SiO_2 derived from siloxene as high performance anode for Li-ion batteries, *Nano Energy*, 2017, **39**, 546–553.
9 F. Shi, Z. Song, P. N. Ross, G. A. Somorjai, R. O. Ritchie and K. Komvopoulos, Failure mechanisms of single-crystal silicon electrodes in lithium-ion batteries, *Nat. Commun.*, 2016, **7**, 11886.
10 X. R. Zhuo and H. G. Beom, Size-dependent fracture properties of cracked silicon nanofilms, *Mater. Sci. Eng., A*, 2015, **636**, 470–475.
11 M. T. McDowell, S. W. Lee, J. T. Harris, B. A. Korgel, C. Wang, W. D. Nix and Y. Cui, In situ TEM of two-phase lithiation of amorphous silicon nanospheres, *Nano Lett.*, 2013, **13**, 758–764.
12 V. Baranchugov, E. Markevich, E. Pollak, G. Salitra and D. Aurbach, Amorphous silicon thin films as a high capacity anodes for Li-ion batteries in ionic liquid electrolytes, *Electrochem. Commun.*, 2007, **9**, 796–800.
13 C. C. Nguyen and S.-W. Song, Interfacial structural stabilization on amorphous silicon anode for improved cycling performance in lithium-ion batteries, *Electrochim. Acta*, 2010, **55**, 3026–3033.
14 L. Zhang, L. Zhang, L. Chai, P. Xue, W. Hao and H. Zheng, A coordinatively cross-linked polymeric network as a functional binder for high-performance silicon submicroparticle anodes in lithium-ion batteries, *J. Mater. Chem. A*, 2014, **2**, 19036–19045.
15 C. Xu, F. Lindgren, B. Philippe, M. Gorgoi, F. Björefors, K. Edström and T. Gustafsson, Improved Performance of the Silicon Anode for Li-Ion Batteries: Understanding the Surface Modification Mechanism of Fluoroethylene Carbonate as an Effective Electrolyte Additive, *Chem. Mater.*, 2015, **27**, 2591–2599.
16 A. Casimir, H. G. Zhang, O. Ogoke, J. C. Amine, J. Lu and G. Wu, Silicon-based anodes for lithium-ion batteries: effectiveness of materials synthesis and electrode preparation, *Nano Energy*, 2016, **27**, 359–376.
17 Y. T. Jin, N. J. H. Kneusels, P. C. M. M. Magusin, G. Kim, E. Castillo-Martinez, L. E. Marbella, R. N. Kerber, D. J. Howe, S. Paul, T. Liu and C. P. Grey, Identifying the Structural Basis for the Increased Stability of the Solid Electrolyte Interphase Formed on Silicon with the Additive

Fluoroethylene Carbonate, *J. Am. Chem. Soc.*, 2017, **139**, 14992–15004.

18 M. Ulldemolins, F. Le Cras, B. Pecquenard, V. P. Phan, L. Martin and H. Martinez, Investigation on the part played by the solid electrolyte interphase on the electrochemical performance of the silicon electrode for lithium-ion batteries, *J. Power Sources*, 2012, **206**, 245–252.

19 L. B. Chen, K. Wang, X. H. Xie and J. Y. Xie, Effect of vinylene carbonate (VC) as electrolyte additive on electrochemical performance of Si film anode for lithium ion batteries, *J. Power Sources*, 2007, **174**, 538–543.

20 A. Rezqita, M. Sauer, A. Foelske, H. Kronberger and A. Trifonova, The effect of electrolyte additives on electrochemical performance of silicon/mesoporous carbon (Si/MC) for anode materials for lithium-ion batteries, *Electrochim. Acta*, 2017, **247**, 600–609.

21 A. Schiele, B. Breitung, T. Hatsukade, B. B. Berkes, P. Hartmann, J. Janek and T. Brezesinski, The Critical Role of Fluoroethylene Carbonate in the Gassing of Silicon Anodes for Lithium-Ion Batteries, *ACS Energy Lett.*, 2017, **2**, 2228–2233.

22 Y. M. Lin, K. C. Klavetter, P. R. Abel, N. C. Davy, J. L. Snider, A. Heller and C. B. Mullins, High performance silicon nanoparticle anode in fluoroethylene carbonate-based electrolyte for Li-ion batteries, *Chem. Commun.*, 2012, **48**, 7268–7270.

23 G. B. Han, M. H. Ryou, K. Y. Cho, Y. M. Lee and J. K. Park, Effect of succinic anhydride as an electrolyte additive on electrochemical characteristics of silicon thin-film electrode, *J. Power Sources*, 2010, **195**, 3709–3714.

24 Y. Li, G. J. Xu, Y. F. Yao, L. G. Xue, S. Zhang, Y. Lu, O. Toprakci and X. W. Zhang, Improvement of cyclability of silicon-containing carbon nanofiber anodes for lithium-ion batteries by employing succinic anhydride as an electrolyte additive, *J. Solid State Electrochem.*, 2013, **17**, 1393–1399.

25 M. Q. Li, M. Z. Qu, X. Y. He and Z. L. Yu, Electrochemical Performance of Si/Graphite/Carbon Composite Electrode in Mixed Electrolytes Containing LiBOB and $LiPF_6$, *J. Electrochem. Soc.*, 2009, **156**, A294–A298.

26 K. Schroder, J. Avarado, T. A. Yersak, J. C. Li, N. Dudney, L. J. Webb, Y. S. Meng and K. J. Stevenson, The Effect of Fluoroethylene Carbonate as an Additive on the Solid Electrolyte Interphase on Silicon Lithium-Ion Electrodes, *Chem. Mater.*, 2015, **27**, 5531–5542.

27 N. S. Choi, K. H. Yew, K. Y. Lee, M. Sung, H. Kim and S. S. Kim, Effect of fluoroethylene carbonate additive on interfacial properties of silicon thin-film electrode, *J. Power Sources*, 2006, **161**, 1254–1259.

28 I. A. Profatilova, C. Stock, A. Schmitz, S. Passerini and M. Winter, Enhanced thermal stability of a lithiated nano-silicon electrode by fluoroethylene carbonate and vinylene carbonate, *J. Power Sources*, 2013, **222**, 140–149.

29 Y. Horowitz, H. L. Han, F. A. Soto, W. T. Ralston, P. B. Balbuena and G. A. Somorjai, Fluoroethylene Carbonate as a Directing Agent in Amorphous Silicon Anodes: Electrolyte Interface Structure Probed by Sum Frequency Vibrational Spectroscopy and Ab Initio Molecular Dynamics, *Nano Lett.*, 2018, **18**, 1145–1151.

30 Y. Horowitz, H. G. Steinruck, H. L. Han, C. Cao, Abate II, Y. Tsao, M. F. Toney and G. A. Somorjai, Fluoroethylene Carbonate Induces Ordered Electrolyte Interface on Silicon and Sapphire Surfaces as Revealed by Sum Frequency Generation Vibrational Spectroscopy and X-ray Reflectivity, *Nano Lett.*, 2018, **18**, 2105–2111.

31 G. M. Veith, M. Doucet, R. L. Sacci, B. Vacaliuc, J. K. Baldwin and J. F. Browning, Determination of the Solid Electrolyte Interphase Structure Grown on a Silicon Electrode Using a Fluoroethylene Carbonate Additive, *Sci. Rep.*, 2017, **7**, 6326.

32 W. J. Tang, W. J. Peng, G. C. Yan, H. J. Guo, X. H. Li and Y. Zhou, Effect of fluoroethylene carbonate as an electrolyte additive on the cycle performance of silicon-carbon composite anode in lithium-ion battery, *Ionics*, 2017, **23**, 3281–3288.

33 R. Jung, M. Metzger, D. Haering, S. Solchenbach, C. Marino, N. Tsiouvaras, C. Stinner and H. A. Gasteiger, Consumption of Fluoroethylene Carbonate (FEC) on Si-C Composite Electrodes for Li-Ion Batteries, *J. Electrochem. Soc.*, 2016, **163**, A1705–A1716.

34 H. Jo, J. Kim, D. T. Nguyen, K. K. Kang, D. M. Jeon, A. R. Yang and S. W. Song, Stabilizing the Solid Electrolyte Interphase Layer and Cycling Performance of Silicon-Graphite Battery Anode by Using a Binary Additive of Fluorinated Carbonates, *J. Phys. Chem. C*, 2016, **120**, 22466–22475.

35 T. Y. Ma, X. N. Yu, X. L. Cheng, H. Y. Li, W. T. Zhu and X. P. Qiu, Confined Solid Electrolyte Interphase Growth Space with Solid Polymer Electrolyte in Hollow Structured Silicon Anode for Li-Ion Batteries, *ACS Appl. Mater. Interfaces*, 2017, **9**, 13247–13254.

36 V. Chakrapani, F. Rusli, M. A. Filler and P. A. Kohl, Quaternary Ammonium Ionic Liquid Electrolyte for a Silicon Nanowire-Based Lithium Ion Battery, *J. Phys. Chem. C*, 2011, **115**, 22048–22053.

37 M. Q. Xu, L. S. Hao, Y. L. Liu, W. S. Li, L. D. Xing and B. Li, Experimental and Theoretical Investigations of Dimethylacetamide (DMAc) as Electrolyte Stabilizing Additive for Lithium Ion Batteries, *J. Phys. Chem. C*, 2011, **115**, 6085–6094.

38 A. Xiao, W. T. Li and B. L. Lucht, Thermal reactions of mesocarbon microbead (MCMB) particles in $LiPF_6$-based electrolyte, *J. Power Sources*, 2006, **162**, 1282–1288.

39 Y. S. Zhang, C. Li, X. X. Cai, J. S. Yao, M. Li, X. Zhang and Q. Z. Liu, High alkaline tolerant electrolyte membrane with improved conductivity and mechanical strength *via* lithium chloride/dimethylacetamide dissolved microcrystalline cellulose for Zn–Air batteries, *Electrochim. Acta*, 2016, **220**, 635–642.

40 W. Walker, V. Giordani, J. Uddin, V. S. Bryantsev, G. V. Chase and D. Addison, A Rechargeable LiO_2 Battery Using a Lithium Nitrate/*N*,*N*-Dimethylacetamide Electrolyte, *J. Am. Chem. Soc.*, 2013, **135**, 2076–2079.

41 V. Giordani, J. Uddin, V. S. Bryantsev, G. V. Chase and D. Addison, High Concentration Lithium Nitrate/

Dimethylacetamide Electrolytes for Lithium/Oxygen Cells, *J. Electrochem. Soc.*, 2016, **163**, A2673–A2678.

42 W. Wieczorek, A. Zalewska, D. Raducha, Z. Florjanczyk, J. R. Stevens, A. Ferry and P. Jacobsson, Polyether, poly(*N*,*N*-dimethylacrylamide), and $LiClO_4$ composite polymeric electrolytes, *Macromolecules*, 1996, **29**, 143–155.

43 S. A. Dobrowski, G. R. Davies, J. E. Mcintyre and I. M. Ward, Ionic-Conduction In Poly(*N*,*N*-Dimethylacrylamide) Gels Complexing Lithium-Salts, *Polymer*, 1991, **32**, 2887–2891.

44 M. S. Donovan, A. B. Lowe and C. L. McCormick, Investigation of the effects of chain transfer agent architecture on the synthesis of near monodisperse poly(*N*,*N*-dimethylacrylamide) *via* RAFT, *Abstr. Pap. Am. Chem. Soc.*, 2001, **222**, U266.

45 J. Scheers, S. Fantini and P. Johansson, A review of electrolytes for lithium-sulphur batteries, *J. Power Sources*, 2014, **255**, 204–218.

46 J. H. Choi, H. J. Lee and S. H. Moon, Effects of electrolytes on the transport phenomena in a cation-exchange membrane, *J. Colloid Interface Sci.*, 2001, **238**, 188–195.

47 C. Xu, F. Lindgren, B. Philippe, M. Gorgoi, F. Bjorefors, K. Edstrom and T. Gustafsson, Improved Performance of the Silicon Anode for Li-Ion Batteries: Understanding the Surface Modification Mechanism of Fluoroethylene Carbonate as an Effective Electrolyte Additive, *Chem. Mater.*, 2015, **27**, 2591–2599.

48 S. Santee, A. Xiao, L. Yang, J. Gnanaraj and B. L. Lucht, Effect of combinations of additives on the performance of lithium ion batteries, *J. Power Sources*, 2009, **194**, 1053–1060.

49 Q. J. Lu, Y. L. Ding, Q. T. Qu, T. Gao, X. L. Zhang, M. Shen and H. H. Zheng, N-Methylacetamide as an electrolyte component for suppressing co-intercalation of propylene carbonate in lithium ion batteries, *RSC Adv.*, 2016, **6**, 65847–65853.

50 J. H. Ryu, J. W. Kim, Y. E. Sung and S. M. Oh, Failure modes of silicon powder negative electrode in lithium secondary batteries, *Electrochem. Solid-State Lett.*, 2004, **7**, A306–A309.

51 Y. Y. Gu, S. M. Yang, G. B. Zhu, Y. N. Yuan, Q. T. Qu, Y. Wang and H. H. Zheng, The effects of cross-linking cations on the electrochemical behavior of silicon anodes with alginate binder, *Electrochim. Acta*, 2018, **269**, 405–414.